Supplement of Earth Syst. Dynam., 11, 737–750, 2020
https://doi.org/10.5194/esd-11-737-2020-supplement


Earth System Dynamics
Open Access

*Supplement of*

# Emergent constraints on transient climate response (TCR) and equilibrium climate sensitivity (ECS) from historical warming in CMIP5 and CMIP6 models

**Femke J. M. M. Nijsse et al.**

*Correspondence to:* Femke J. M. M. Nijsse (f.j.m.m.nijsse@exeter.ac.uk)

| **Centre** | **Model** | **F$_{2x}$** | $\lambda$ | **ECS** | **TCR** | **n** | $\Delta T$ | $d\Delta T$ |
|---|---|---|---|---|---|---|---|---|
| BCC | bcc-csm1-1-m | 3.36 | 1.15 | 2.91 | 2.07 | 1 | 0.97 | |
| BCC | bcc-csm1-1 | 3.70 | 1.27 | 2.91 | 1.76 | 1 | 0.92 | |
| BNU | BNU-ESM | 3.77 | 0.93 | 4.07 | 2.54 | 1 | 0.99 | |
| CCCma | CanESM2 | 3.76 | 1.01 | 3.71 | 2.30 | 5 | 1.16 | 0.05 |
| CMCC | CMCC-CM | | 1.01 | | 1.98 | 1 | 0.75 | |
| CNRM-CERFACS | CNRM-CM5 | 3.32 | 1.01 | 3.28 | 1.97 | 5 | 0.74 | 0.12 |
| CSIRO-BOM | ACCESS1-0 | 4.26 | 1.09 | 3.90 | 1.77 | 1 | 0.70 | |
| CSIRO-BOM | ACCESS1-3 | 3.97 | 1.09 | 3.63 | 1.60 | 1 | 0.79 | |
| CSIRO-QCCCE | CSIRO-Mk3-6-0 | 4.76 | 1.09 | 4.36 | 1.69 | 10 | 0.68 | 0.08 |
| INM | inmcm4 | 1.48 | 0.72 | 2.05 | 1.29 | 1 | 0.42 | |
| IPSL | IPSL-CM5A-LR | 3.13 | 0.77 | 4.05 | 1.97 | 4 | 0.98 | 0.08 |
| IPSL | IPSL-CM5A-MR | | 0.54 | | 1.98 | 1 | 0.93 | |
| IPSL | IPSL-CM5B-LR | 1.43 | 0.54 | 2.64 | 1.44 | 1 | 0.58 | |
| MIROC | MIROC-ESM | 2.58 | 0.54 | 4.75 | 2.01 | 1 | 0.70 | |
| MIROC | MIROC5 | 1.47 | 0.54 | 2.70 | 1.47 | 3 | 0.73 | 0.08 |
| MOHC | HadGEM2-ES | 2.52 | 0.54 | 4.64 | 2.43 | 4 | 0.95 | 0.14 |
| MPI-M | MPI-ESM-LR | 5.48 | 1.49 | 3.66 | 2.01 | 3 | 0.77 | 0.04 |
| MPI-M | MPI-ESM-MR | 2.74 | 0.78 | 3.51 | 2.03 | 1 | 0.84 | |
| MRI | MRI-CGCM3 | 2.04 | 0.78 | 2.61 | 1.52 | 1 | 0.30 | |
| NASA-GISS | GISS-E2-H | 1.89 | 0.78 | 2.43 | 1.78 | 5 | 0.78 | 0.08 |
| NASA-GISS | GISS-E2-R | 2.18 | 0.96 | 2.28 | 1.48 | 5 | 0.64 | 0.11 |
| NCC | NorESM1-ME | | 1.56 | | 1.54 | 1 | 0.66 | |
| NCC | NorESM1-M | 4.57 | 1.56 | 2.93 | 1.39 | 1 | 0.66 | |
| NOAA-GFDL | GFDL-CM3 | 2.45 | 0.61 | 4.03 | 1.76 | 1 | 1.08 | |
| NOAA-GFDL | GFDL-ESM2G | 1.42 | 0.61 | 2.34 | 1.21 | 1 | 0.71 | |
| NOAA-GFDL | GFDL-ESM2M | 1.49 | 0.61 | 2.46 | 1.37 | 1 | 0.63 | |
| NSF-DOE-NCAR | CESM1-BGC | | 0.61 | | 1.71 | 1 | 0.86 | |
| NSF-DOE-NCAR | CESM1-CAM5 | | 1.09 | | 2.29 | 3 | 0.78 | 0.07 |
| | Mean | 2.98 | 0.90 | 3.30 | 1.80 | 2.32 | 0.78 | 0.08 |
| | SD | 0.24 | 0.31 | 0.79 | 0.34 | 2.12 | 0.18 | 0.03 |

**Table S1.** Included CMIP5 models. Values were determined using the Gregory method, consistent with the CMIP6 values.

| **Model** | **ECS** | $\lambda$ | $\mathbf{F}_{2x}$ | **C** | **C0** | $\gamma$ | $\tau_f$ | $\tau_s$ |
|---|---|---|---|---|---|---|---|---|
| AWI-CM-1-1-MR | 3.13 | 1.21 | 3.80 | 6.34 | 51.4 | 0.55 | 3.56 | 138.1 |
| BCC-CSM2-MR | 3.02 | 1.03 | 3.11 | 7.16 | 74.1 | 0.78 | 3.88 | 169.7 |
| BCC-ESM1 | 3.34 | 0.94 | 3.12 | 6.84 | 96.2 | 0.66 | 4.22 | 250.6 |
| CAMS-CSM1-0 | 2.30 | 1.76 | 4.05 | 7.79 | 52.9 | 0.64 | 3.21 | 114.1 |
| FGOALS-f3-L | 3.00 | 1.35 | 4.04 | 7.16 | 71.0 | 0.71 | 3.44 | 154.3 |
| CanESM5 | 5.66 | 0.64 | 3.61 | 6.69 | 73.9 | 0.55 | 5.54 | 255.9 |
| CNRM-CM6-1 | 4.90 | 0.73 | 3.59 | 6.20 | 111.1 | 0.58 | 4.69 | 348.7 |
| CNRM-ESM2-1 | 4.75 | 0.64 | 3.03 | 6.39 | 114.3 | 0.56 | 5.28 | 388.7 |
| ACCESS-CM2 | 4.70 | 0.71 | 3.34 | 6.98 | 86.9 | 0.60 | 5.23 | 271.5 |
| ACCESS-ESM1-5 | 3.86 | 0.74 | 2.85 | 6.31 | 84.2 | 0.72 | 4.24 | 234.9 |
| E3SM-1-0 | 5.31 | 0.63 | 3.34 | 6.83 | 39.7 | 0.43 | 6.29 | 160.6 |
| EC-Earth3-Veg | 4.29 | 0.80 | 3.42 | 6.12 | 38.4 | 0.52 | 4.51 | 124.5 |
| EC-Earth3 | 4.18 | 0.81 | 3.40 | 6.58 | 39.8 | 0.50 | 4.90 | 132.4 |
| INM-CM4-8 | 1.83 | 1.48 | 2.71 | 4.39 | 27.9 | 0.80 | 1.89 | 54.8 |
| INM-CM5-0 | 1.91 | 1.55 | 2.97 | 6.85 | 45.2 | 0.57 | 3.19 | 109.6 |
| IPSL-CM6A-LR | 4.53 | 0.77 | 3.49 | 6.37 | 58.9 | 0.47 | 5.06 | 205.5 |
| MIROC6 | 2.56 | 1.46 | 3.75 | 7.48 | 171.6 | 0.66 | 3.51 | 378.7 |
| HadGEM3-GC31-LL | 5.55 | 0.62 | 3.45 | 6.77 | 72.4 | 0.55 | 5.64 | 252.6 |
| HadGEM3-GC31-MM | 5.44 | 0.63 | 3.44 | 7.10 | 70.4 | 0.65 | 5.40 | 225.7 |
| UKESM1-0-LL | 5.37 | 0.67 | 3.61 | 6.27 | 75.0 | 0.54 | 5.08 | 257.4 |
| MPI-ESM1-2-HR | 2.95 | 1.25 | 3.70 | 6.46 | 81.1 | 0.72 | 3.23 | 178.7 |
| MRI-ESM2-0 | 3.15 | 1.07 | 3.36 | 5.72 | 89.7 | 1.08 | 2.62 | 169.5 |
| GISS-E2-1-G | 2.71 | 1.44 | 3.91 | 5.44 | 142.3 | 0.88 | 2.33 | 261.5 |
| GISS-E2-1-H | 3.08 | 1.18 | 3.62 | 7.23 | 82.5 | 0.66 | 3.89 | 197.4 |
| GISS-E2-2-G | 2.40 | 1.58 | 3.79 | 7.78 | 908.6 | 0.51 | 3.71 | 2340.9 |
| CESM2-WACCM | 4.71 | 0.69 | 3.26 | 5.88 | 79.4 | 0.85 | 3.73 | 212.9 |
| CESM2 | 5.22 | 0.64 | 3.34 | 5.93 | 72.2 | 0.84 | 3.91 | 204.3 |
| NorESM2-LM | 2.56 | 1.33 | 3.42 | 2.94 | 100.6 | 1.09 | 1.21 | 168.5 |
| GFDL-CM4 | 3.91 | 0.80 | 3.15 | 4.87 | 80.3 | 0.72 | 3.15 | 214.4 |
| GFDL-ESM4 | 2.66 | 1.35 | 3.58 | 7.17 | 125.8 | 0.62 | 3.63 | 298.7 |
| NESM3 | 4.69 | 0.82 | 3.85 | 4.93 | 98.4 | 0.48 | 3.77 | 328.6 |
| SAM0-UNICON | 2.83 | 1.06 | 3.01 | 3.26 | 21.5 | 0.75 | 1.75 | 50.4 |

**Table S2.** Values were determined following the algorithm described in Geoffroy et al. (2013a). For models that come close to equilibrium within the first 150 years, we made two slight adjustment to the algorithm allowing parameters to be estimated even in the case that the temperature in a certain year exceeded $2 \times$ ECS. The long time scales (the second estimation step described in Geoffroy et al. (2013a)), were estimated dropping those years after the first instance of a year that exceeded $2 \times$ ECS to avoid taking the logarithm of negative values. Similar problems occurred for a limited number of models when estimating the fast time scale. Here, we used direct least-squares curve-fitting (using the scipy package `curve_fit` function) over the first ten years to estimate the parameter when taking a logarithm was not possible.

| Model | ECS | $\lambda$ | $F_{2x}$ | C | C0 | $\gamma$ | $\tau_f$ | $\tau_s$ | $\epsilon$ |
|---|---|---|---|---|---|---|---|---|---|
| AWI-CM-1-1-MR | 3.28 | 1.27 | 4.17 | 7.03 | 51.35 | 0.55 | 3.65 | 177.07 | 1.33 |
| BCC-CSM2-MR | 3.19 | 1.07 | 3.42 | 7.95 | 74.09 | 0.78 | 3.97 | 205.55 | 1.26 |
| BCC-ESM1 | 3.63 | 0.93 | 3.39 | 7.46 | 96.15 | 0.66 | 4.27 | 323.42 | 1.29 |
| CAMS-CSM1-0 | 2.38 | 1.86 | 4.43 | 8.67 | 52.86 | 0.64 | 3.32 | 146.40 | 1.33 |
| FGOALS-f3-L | 3.29 | 1.42 | 4.68 | 8.46 | 70.97 | 0.71 | 3.57 | 230.34 | 1.56 |
| CanESM5 | 5.77 | 0.66 | 3.80 | 6.83 | 75.11 | 0.55 | 5.40 | 274.38 | 1.08 |
| CNRM-CM6-1 | 5.08 | 0.73 | 3.69 | 6.39 | 111.14 | 0.58 | 4.70 | 385.93 | 1.10 |
| CNRM-ESM2-1 | 4.40 | 0.65 | 2.87 | 6.04 | 114.27 | 0.56 | 5.26 | 315.70 | 0.82 |
| ACCESS-CM2 | 5.56 | 0.68 | 3.79 | 7.95 | 86.93 | 0.60 | 5.29 | 410.60 | 1.48 |
| ACCESS-ESM1-5 | 4.76 | 0.73 | 3.46 | 7.77 | 84.18 | 0.72 | 4.38 | 391.60 | 1.66 |
| E3SM-1-0 | 5.83 | 0.63 | 3.68 | 7.57 | 39.65 | 0.43 | 6.44 | 222.54 | 1.41 |
| EC-Earth3-Veg | 4.57 | 0.85 | 3.89 | 7.04 | 38.38 | 0.52 | 4.67 | 162.52 | 1.41 |
| EC-Earth3 | 4.41 | 0.85 | 3.76 | 7.34 | 39.84 | 0.50 | 5.03 | 167.79 | 1.34 |
| INM-CM4-8 | 1.85 | 1.67 | 3.10 | 5.35 | 27.89 | 0.80 | 2.08 | 61.91 | 1.28 |
| INM-CM5-0 | 1.98 | 1.63 | 3.22 | 7.58 | 45.23 | 0.57 | 3.31 | 140.28 | 1.31 |
| IPSL-CM6A-LR | 4.91 | 0.77 | 3.79 | 6.95 | 58.95 | 0.47 | 5.12 | 271.14 | 1.33 |
| MIROC6 | 2.70 | 1.44 | 3.87 | 7.73 | 171.58 | 0.66 | 3.51 | 458.47 | 1.18 |
| HadGEM3-GC31-LL | 6.00 | 0.62 | 3.71 | 7.29 | 72.38 | 0.55 | 5.69 | 310.24 | 1.23 |
| HadGEM3-GC31-MM | 5.64 | 0.64 | 3.59 | 7.45 | 70.44 | 0.65 | 5.44 | 249.61 | 1.12 |
| UKESM1-0-LL | 5.65 | 0.67 | 3.80 | 6.61 | 75.96 | 0.54 | 5.11 | 297.04 | 1.16 |
| MPI-ESM1-2-HR | 3.21 | 1.33 | 4.26 | 7.55 | 81.08 | 0.72 | 3.32 | 247.80 | 1.47 |
| MRI-ESM2-0 | 3.33 | 1.18 | 3.94 | 6.95 | 89.72 | 1.08 | 2.76 | 202.70 | 1.32 |
| GISS-E2-1-G | 2.76 | 1.46 | 4.02 | 5.64 | 142.31 | 0.88 | 2.35 | 278.99 | 1.07 |
| GISS-E2-1-H | 3.19 | 1.19 | 3.80 | 7.62 | 82.46 | 0.66 | 3.93 | 225.62 | 1.16 |
| GISS-E2-2-G | 2.08 | 1.79 | 3.72 | 7.65 | 908.63 | 0.51 | 3.71 | 969.30 | 0.50 |
| CESM2-WACCM | 5.61 | 0.73 | 4.08 | 7.54 | 79.42 | 0.85 | 3.92 | 321.55 | 1.60 |
| CESM2 | 6.44 | 0.67 | 4.30 | 7.86 | 72.19 | 0.84 | 4.15 | 331.02 | 1.71 |
| NorESM2-LM | 2.95 | 1.69 | 4.98 | 4.47 | 100.55 | 1.09 | 1.29 | 261.79 | 1.93 |
| GFDL-CM4 | 4.84 | 0.85 | 4.10 | 6.50 | 80.33 | 0.72 | 3.31 | 372.34 | 1.84 |
| GFDL-ESM4 | 2.73 | 1.35 | 3.67 | 7.36 | 125.75 | 0.62 | 3.63 | 332.29 | 1.11 |
| NESM3 | 4.69 | 0.82 | 3.85 | 4.93 | 98.38 | 0.48 | 3.77 | 329.87 | 1.00 |
| SAM0-UNICON | 2.84 | 1.12 | 3.19 | 3.31 | 21.53 | 0.75 | 1.63 | 49.86 | 1.09 |

**Table S3.** Values were determined following the algorithm described in Geoffroy et al. (2013b). The same modifications to the algorithm were made as in Table S2.

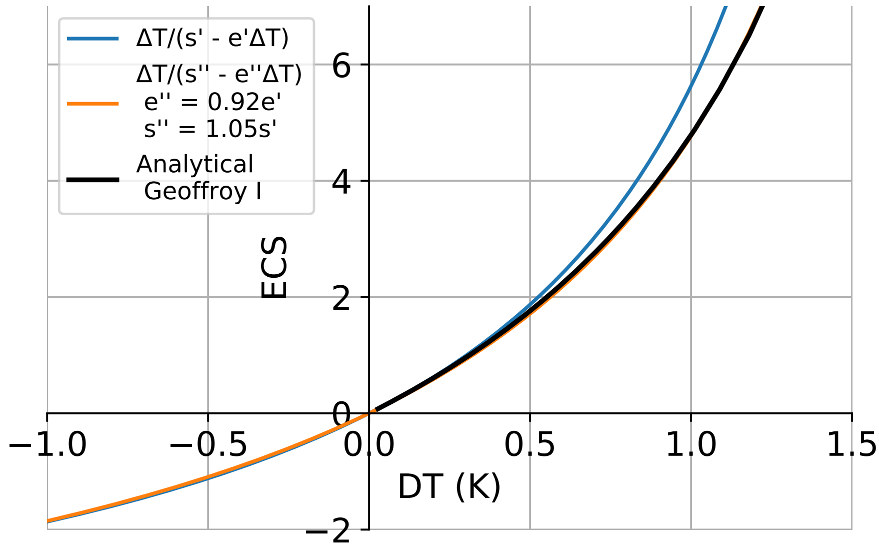


**Supplementary Figure 1.** Comparison of two functions describing the relationship between observed warming and climate sensitivity. The analytical function (black) corresponding to Equation 14 in Geoffroy et al. (2013a), not only depends on $\gamma$ and the forcing, but also on the heat capacity of the two layers, for which typical values were chosen of $C = 8$ and $C_0 = 100$. The linear forcing was $1/140 F_2 x$, and the function was evaluated between year 20 and 70, to cancel transient effects. The parameter $s'$ was chosen to be 5/14, and $e'$ is 0.18. The blue and orange lines are both drawn using $\mathrm{ECS} = \Delta T/(s' - e'\Delta T)$, where in the latter case, the parameters are chosen to approximate the full equation as closely as possible.

## References


Geoffroy, O., Saint-martin, D., Olivié, D. J., Voldoire, A., Bellon, G., and Tytéca, S.: Transient climate response in a two-layer energy-balance model. Part I: Analytical solution and parameter calibration using CMIP5 AOGCM experiments, Journal of Climate, 26, 1841–1857, https://doi.org/10.1175/JCLI-D-12-00195.1, 2013a.

Geoffroy, O., Saint-Martin, D., Bellon, G., Voldoire, A., Olivié, D. J., and Tytéca, S.: Transient climate response in a two-layer energy-balance model. Part II: Representation of the efficacy of deep-ocean heat uptake and validation for CMIP5 AOGCMs, Journal of Climate, 26, 1859–1876, https://doi.org/10.1175/JCLI-D-12-00196.1, 2013b.